ANL-ART-222
ANL-METL-31

Mutual Inductance Level Sensor for Use in Liquid Metals

Nuclear Sciences and Engineering Division

ANL-ART-222
ANL-METL-31

Mutual Inductance Level Sensor for Use in Liquid Metals

E. Kent, C. Grandy

Nuclear Sciences and Engineering Division
Argonne National Laboratory

April 2021

TABLE OF CONTENTS

LIST OF FIGURES

1. Executive Summary

Electromagnetic instrumentation capable of measuring the level of liquid metal has been developed at Argonne National Laboratory's (ANL) Mechanisms Engineering Test Loop (METL). The mutual inductance level sensor (MILS) utilizes the electromagnetic coupling between two coil conductors and a surrounding liquid metal to determine the level of the liquid metal. Mineral insulated cables wrapped on a stainless steel core provide a durable sensor construction. The use of a sealed stainless steel thimble isolates the sensor from the high-temperature liquid metal, allowing for easy sensor maintenance. Modern digital electronics allow for reliable and accurate operation of the sensor. Two sensor variations have been designed and fabricated, and the first variation has seen extensive testing in a non-sodium testing stand as well as in the high-temperature sodium environment of METL. Electromagnetic finite-element analysis studies have been performed using the COMSOL Magnetic Fields Solver. Regular operation of the MILS will commence following in-situ calibration of the sensors in the METL environment.

2. Introduction

A sensor system of particular interest for use in sodium fast reactors (SFR) is a liquid level sensor capable of operating in high-temperature liquid sodium. Traditional methods such as float, sight glass, and differential pressure level indicators have been investigated and found to be incompatible with the high-temperature sodium environment. The preferred method used in past SFR technology relies on electromagnetic interaction with the electrically conductive liquid metal. Attempts were made to purchase such a system, but the historic suppliers no longer manufacture this technology. Therefore, a revitalization effort was needed to bring these sensors back into use. This paper describes the design and testing of modern mutual inductance level sensors (MILS) that offer a non-contact, high-temperature option capable of making continuous measurements over a wide range. The sensors described in this paper are intended for use in sodium systems, but the operation would be nearly identical in other electrically conductive fluids.

3. Theory of Operation

In general, a coil with N_1 turns, cross-sectional area A, and length L that is excited with a time varying current $i_1(t)$ generates a time varying magnetic field $B_1(t)$ inside the coil according to the following equation:

$$B_1(t) = \mu_0 \, {}^{N_1}/_{L} \, i_1(t) \tag{1}$$

Where μ_0 is the permeability of free space characteristic of a vacuum.

If a second coil with N_2 turns is located on the same axis as the first coil, the magnetic flux φ_2 through coil 2 is described by the following equation:

$$\varphi_2(t) = N_2 B_1(t) A \tag{2}$$

When the excitation current varies with time, the flux also varies with time and an induced electromotive force (emf) is generated in the second coil according to the following equation:

$$\varepsilon_2 = {d\varphi_2}/{dt} = -\mu_0 {N_1 N_2}/{L} A {di_1}/{dt} \tag{4}$$

The above equation leads to the definition of mutual inductance of two coaxial coils in a vacuum, now described by the following equation:

$$M = \mu_0 {N_1 N_2}/{L} A \tag{4}$$

Because the sensor does not operate in a vacuum, but rather some arbitrary material, the above equations should be modified where the permeability of free space is replaced with the permeability of the surrounding material. Material specific permeability is given by the following equation:

$$\mu = \mu_0(1 + \chi_m) \tag{5}$$

Where χ_m is the magnetic susceptibility of the material traversed by the magnetic field.

Reference 1 and reference 2 were used for the above equations. Were this sensor to operate alone in a vacuum, Equation 4 would give a direct prediction of the open circuit voltage. If the sensor was located in a homogenous material, Equation 4 with Equation 5 substituted in for the permeability of free space would give a direct prediction of the open circuit voltage. The utility of this sensor emerges when the coils are located near electrically conductive material. As the magnetic field travels out of the coil center and into any surrounding material that is electrically conductive, eddy currents are generated in the conductive material. These eddy currents induce their own magnetic fields that collectively act to resist the original field generated by the coil. This results in a reduced magnetic field associated with the sensor, and therefore a reduced emf in the secondary coil.

This phenomenon is utilized in practice by positioning the sensor such that it is surrounded by liquid sodium. The primary coil is excited with a constant current AC signal, and the secondary coil is connected to a digital multimeter (DMM) that is measuring AC voltage. As the sensor's magnetic field travels through the nearby sodium, eddy currents are generated in the sodium that act to diminish the sensors magnetic field. This is observed as a reduction in output voltage from the secondary coil. An inverse linear relationship between sodium level and output voltage can be observed. Figure 1 shows a simplified diagram of the MILS in operation.

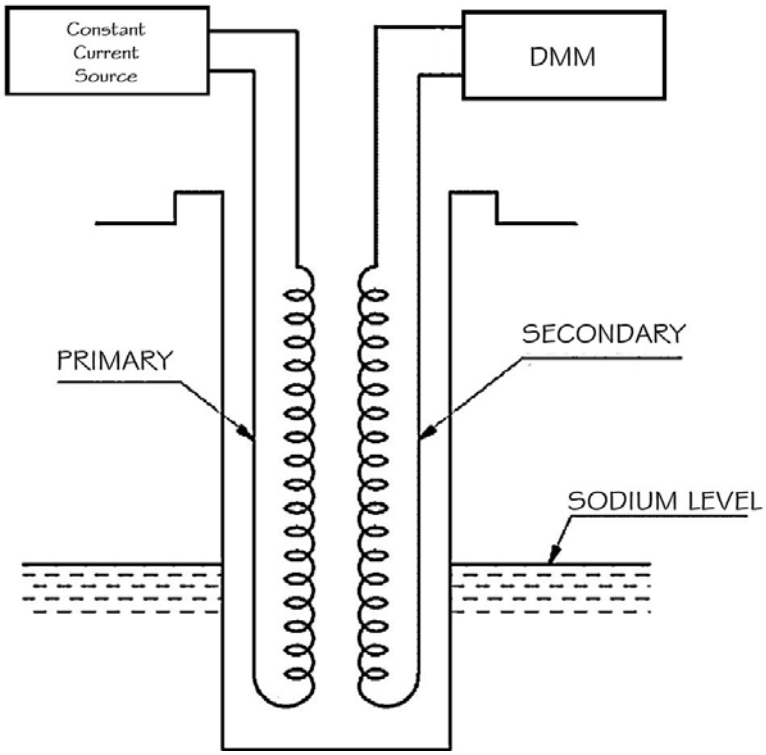

Figure 1: Simplified diagram of mutual inductance level sensor in operation.

4. Preliminary Sensor Design

A series of hand wrapped prototypes were constructed and tested at ANL in the previous few fiscal years [3]. This prototyping and testing was conducted to better understand the theory of operation of MILS technology. The first sensor consisted of two ceramic-coated nickel wires wound on an alumina core with the wrapping of the wires done in a bifilar fashion. An alumina core was chosen as the material is effectively non-conductive and non-magnetic so it would not affect the magnetic field generated during operation. Ceramic-coated nickel wires were chosen as the conductors as the material can operate at temperatures above 650°C which is prototypic of SFR operation. Once constructed, this sensor was tested by conducting a mock calibration. This consisted of energizing one coil (primary coil) with an AC signal from a signal generator and measuring the open circuit voltage generated across the leads of the second coil (secondary coil) using an oscilloscope. Then an aluminum 6061 (Al6061) cylinder was positioned such that the

cylinder covered a bottom segment of the sensor, and the change in signal from the secondary was observed. Al6061 was determined to be an appropriate sodium analog due to the similarities in electromagnetic skin depth when compared to sodium. Sodium at 100°C = 3.19mm [4] and Al-6061 at room temperature = 3.45mm [5]. The Al6061 cylinder was then moved to cover more of the sensor, and the new signal was observed. This was repeated until the sensor was completely surrounded by the Al6061 cylinder with signal measurements taken at every increment. Example data taken using the ceramic MILS is presented in Figure 2.

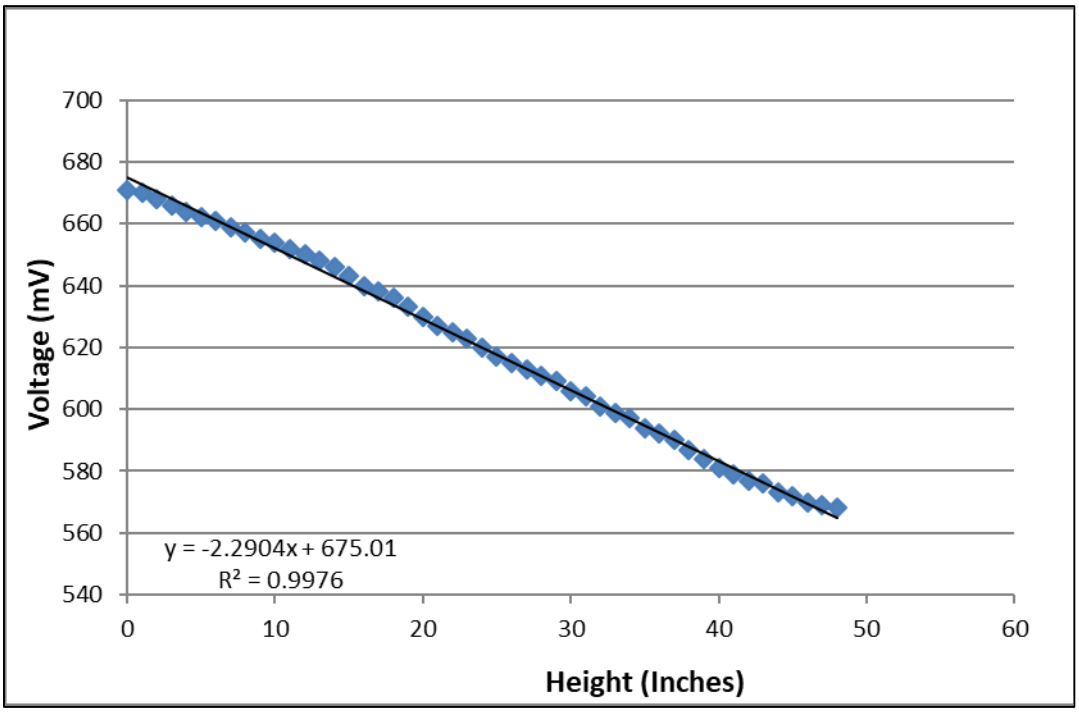

Figure 2: Mock calibration data collected using the first prototype MILS.

While the above data showed good linearity, problems arose when testing the repeatability of the first prototype. Repeated testing produced data that was acceptably linear, but there would be a significant offset in the measured signal voltage when compared to previous tests. It was determined that the ceramic coating on the nickel wires that acted as insulation was not performing effectively, leading to shorts across coil loops. This meant the number of active coils on the sensor was changing unpredictably. This required a redesign using more durable conductor insulation. Additionally, the fragility of the alumina core proved to be troublesome with a number of breaks occurring over the course of operation. This suggested a redesign with a more durable core material.

A second prototype design consisted of nickel-clad copper (NCC) wires with mica insulation wrapped on a stainless steel core. The NCC wires had thick mica insulation and could operate at temperature up to 550°C. The stainless steel core was far more durable than the alumina and is relatively non-magnetic, with a relative permeability value near unity [6]. This means that

while the core material was metallic and conductive, it would not interact much with the magnetic field generated by the sensor. Figure 3 shows the electromagnetic skin depth of stainless steel as a function of frequency. This guides the selection of operating frequency as the skin depth drops exponentially as the operating frequency is increased.

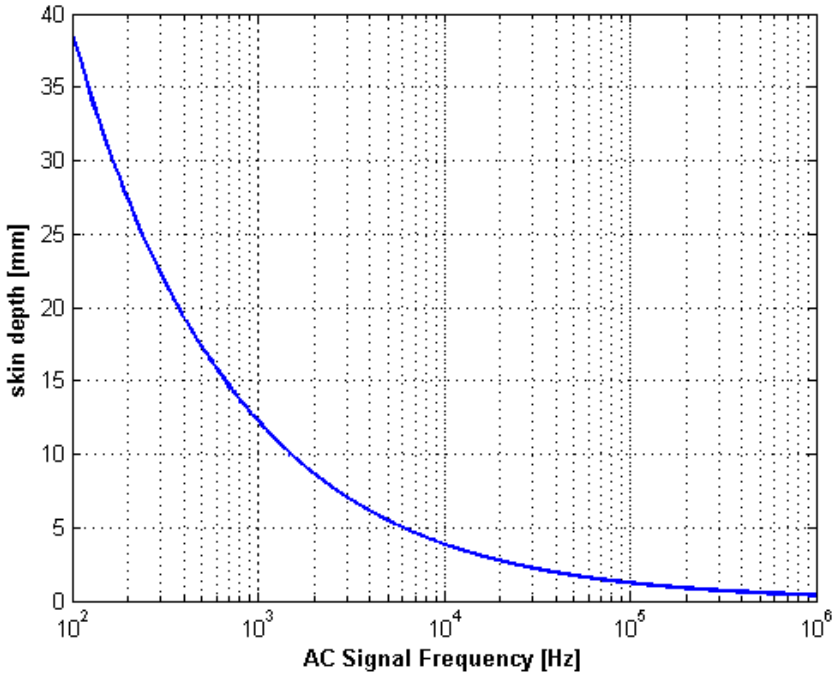

Figure 3: Electromagnetic Skin Depth in Stainless Steel as a Function of Excitation Frequency [2,5,6].

A consequence of using the thicker mica-insulated wires was a reduction in coil wrap count, which leads to a proportional reduction in sensor signal. The wrapping method was altered to counter this coil count reduction, and a two-layer wrap was used where the primary is wrapped first in one layer and the secondary is wrapped on top of the primary to make the second layer. A mock calibration was performed with the second prototype and example data is presented in Figure 4.

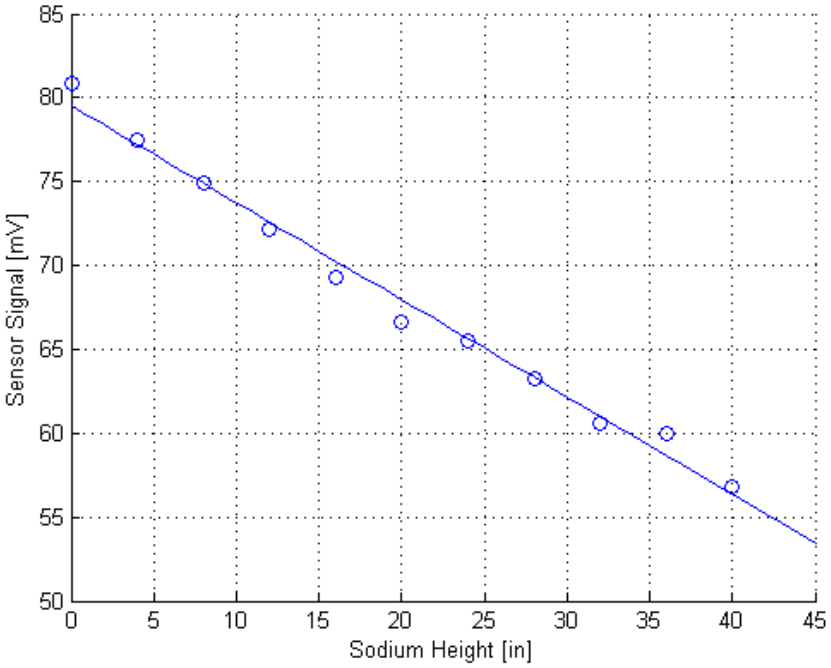

Figure 4: Mock calibration data collected using the second prototype MILS.

The data again showed acceptable linearity, but the signal strength was greatly reduced. The effect of increasing the wire and insulation diameter was only slightly counteracted by the change to two-layer wrapping. As high sensitivity is desired, a new prototype with smaller wires and insulation was designed. Issues with electrical isolation were also experienced with the second prototype, but this was more easily managed with the better insulated wires.

The third prototype sensor used smaller diameter constantan wire with a thin fiberglass insulation. The move to constantan conductor material was made to potentially deal with temperature effects that would be encountered in the future, as constantan has a low temperature coefficient of resistivity when compared to other conductor materials. The two-layer wrapping was used again to maximize the sensor's wrap count. A mock calibration was again performed and the data is presented in Figure 5.

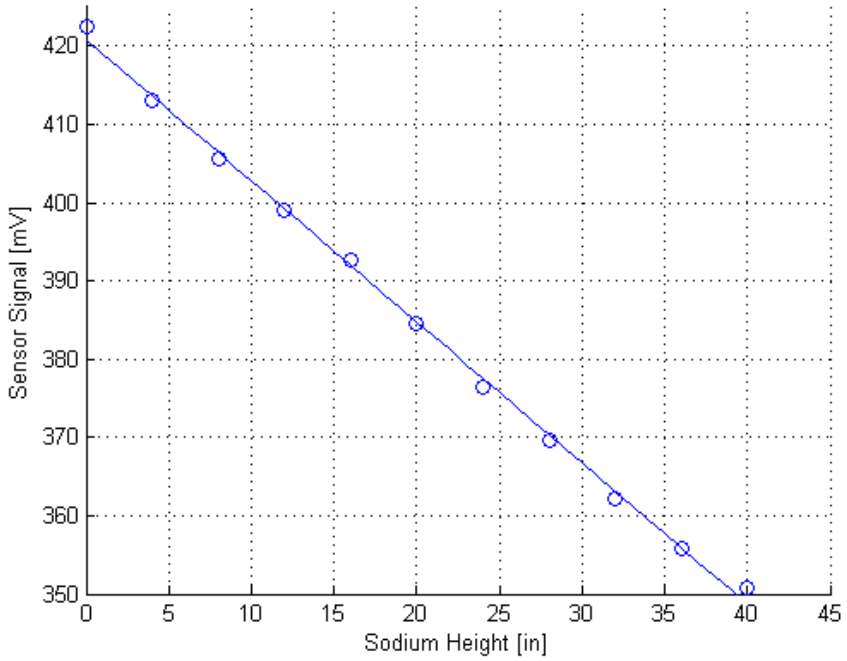

Figure 5: Mock calibration data collected using the third prototype MILS.

The third prototype showed better linearity and increased signal strength when compared to the second prototype. But again issues with electrical isolation were encountered with the third prototype. Handling the sensor and temperature testing the sensor significantly degraded the coils insulation. As these sensors need to be robust to minimize the required maintenance, a significant change in design was required. Figure 6 shows the three prototype next to each other to compare the wrapping and conductor differences.

Figure 6: Progression of MILS prototyping with the ceramic-nickel prototype (left), NCC-mica prototype (mid), and constantan-fiberglass prototype (right) .

5. Current Sensor Design

Maintaining electrical isolation of the sensor coils proved to be the main issue when testing all the hand wrapped prototypes. To address this, mineral-insulated (MI) cable was used in place of the traditionally insulated wires. MI cable with two copper conductors insulated with magnesium-oxide (MgO) inside of a stainless steel sheath was selected for the MILS-MK-I design. A two conductor cable was selected as the manufacturer had this on-hand, and it would simplify the wrapping of the coil on the core. The sensor diameter was selected to fit in the 1-inch ID stainless steel tube used in the METL thimbles. A 70-inch long sensor was designed for use in the METL Expansion Tank, and a 40-inch long sensor was designed for use in the METL Dump Tank. The MI cable used in each sensor is capable of operating up to 1000°F/538°C according to the cable manufacturer. Thermocouple (TC) connectors with copper leads were used to terminate the coils as the MI cable is commonly used for TC probes. Figure 7 shows the 40-inch variation of the MILS-MK-I.

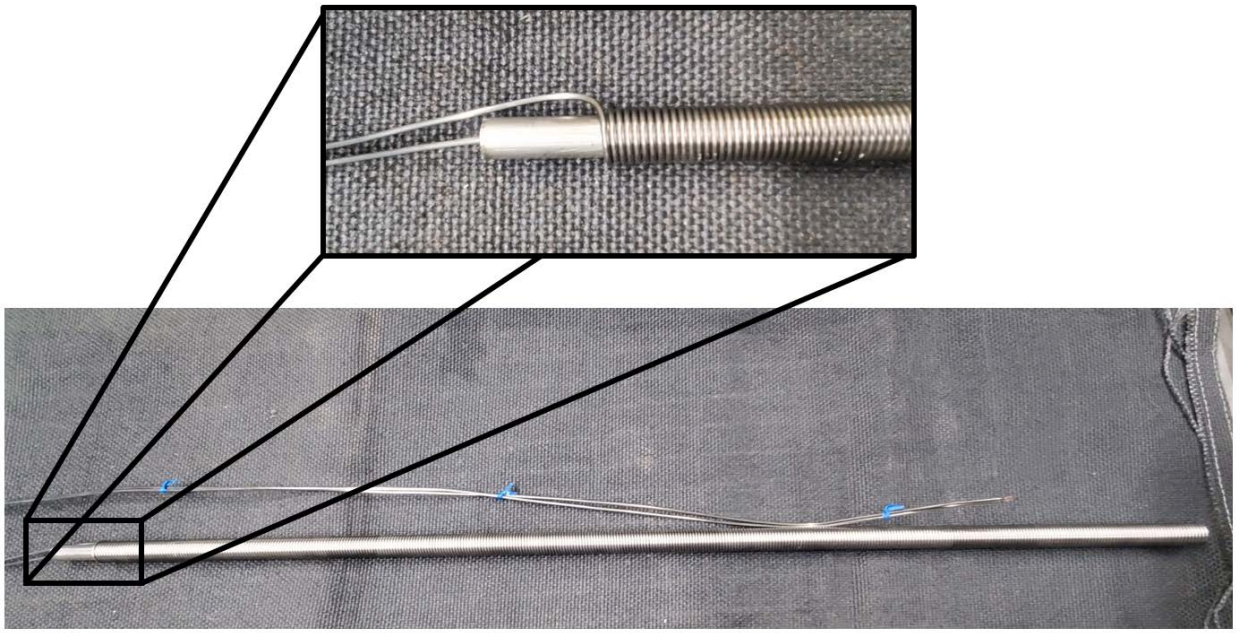

Figure 7: MILS-MK-I

6. Experimental Setup

Testing was performed at ANL at the Mechanisms Engineering Test Loop (METL). METL is an intermediate-scale sodium test facility where sensors and components designed for SFRs can be tested in a prototypic sodium environment [7]. Before testing can be performed in METL, all sensors/components/articles need to be fully qualified in a non-sodium environment. This ensures that the system is working as intended before being introduced to the sodium environment, potentially avoiding expensive time delays or damage to the facility. To accomplish the qualification for the MILS, a non-sodium test stand was fabricated at the METL facility.

The test stand (Figure 8) consists of a stainless steel tube the same dimensions as the sensor thimble, aluminum cylinders surrounding the tube that act as a sodium analog, a cable and winch system to change the position of the sensor with respect to the aluminum (mimicking a change in sodium level), heaters and insulation, and a LabVIEW based data acquisition system. The use of this test stand allows for mock calibration of the MILS over a maximum level change of 40 inches. The heaters and insulation are included to allow for elevated temperature testing in the future.

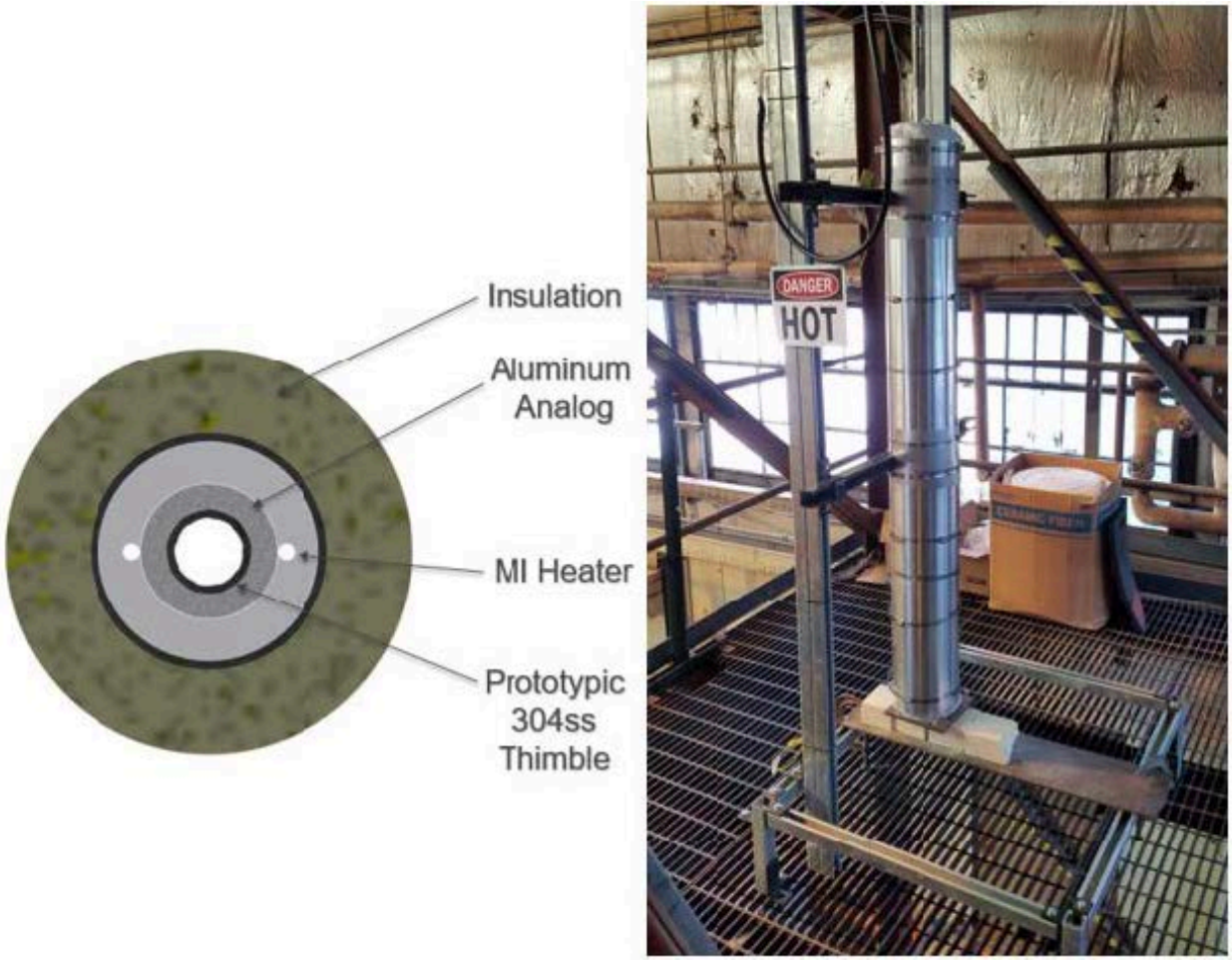

Figure 8: Level Sensor Testing Stand in Building 308 (right). Cross-section view of Testing Stand (left).

The main improvement of the modern MILS system is the inclusion of high precision digital electronics. Previous researchers were limited to analog electronics, and the calibration and maintenance of these systems was a major factor in the performance of their designs [8]. The sensor tested in this work used a digital signal generator, constant current amplifier, and a power resistor to drive a constant current AC signal at sub-RF frequencies. It is preferable to drive the sensor with a constant current signal as this helps compensate for any impedance changes due to changes in temperature. The secondary is read using a high precision digital multimeter capable of making real-RMS voltage measurements.

The testing procedure mimics a full scale calibration of the sensor over 40 inches of level change [9]. To begin, the sensor is full inserted into the test stand so that the active length of the sensor "sees" 40 inches of metal. The electronics are powered on and a LabVIEW program is used to collect data at regular time intervals. After sufficient data is collected at this bottom position, the sensor is raised by 10% full scale (4") using the winch system and data collection resumes.

This is repeated for the full scale of the test stand. The data can then be processed into a calibration curve, where the "sodium" level is compared to the secondary output voltage.

7. FEA Model and Studies

Parallel to the experimental work, analysis work was completed using the COMSOL Magnetic Fields Solver. The development of a validated model allows for rapid testing of design changes, and the relatively simple geometry of the test stand and sensor lend themselves to FEA modeling. The test stand and sensor both have cylindrical geometry, so a 2-D axisymmetric model was drafted in AutoCAD and imported into the COMSOL environment. The Magnetic Fields Solver has a built in coil analysis tool that makes modeling electrical coils simple. The material properties used in the solver are the electrical conductivity, relative permeability, and relative permittivity.

A preliminary model was generated using the known geometry of the system, the known operating conditions, and material properties taken from literature [4,5,6,10]. This model was solved as a sanity check to observe if the solved magnetic field intensities match what is expected in reality. Figure 9 shows a COMSOL generated map of the magnetic field intensity with the sensor positioned such that it is half covered by the Al6061 (the sensor "sees" 20-inches of process metal). The center of the sensor core is at r=0, and we see a strong magnetic field inside the sensor as expected. The magnetic field lines in white that propagate from the outside of the sensor are seen to be collected by the Al6061 cylinder, as expected. This give initial confidence that the physics are working as expected in COMSOL.

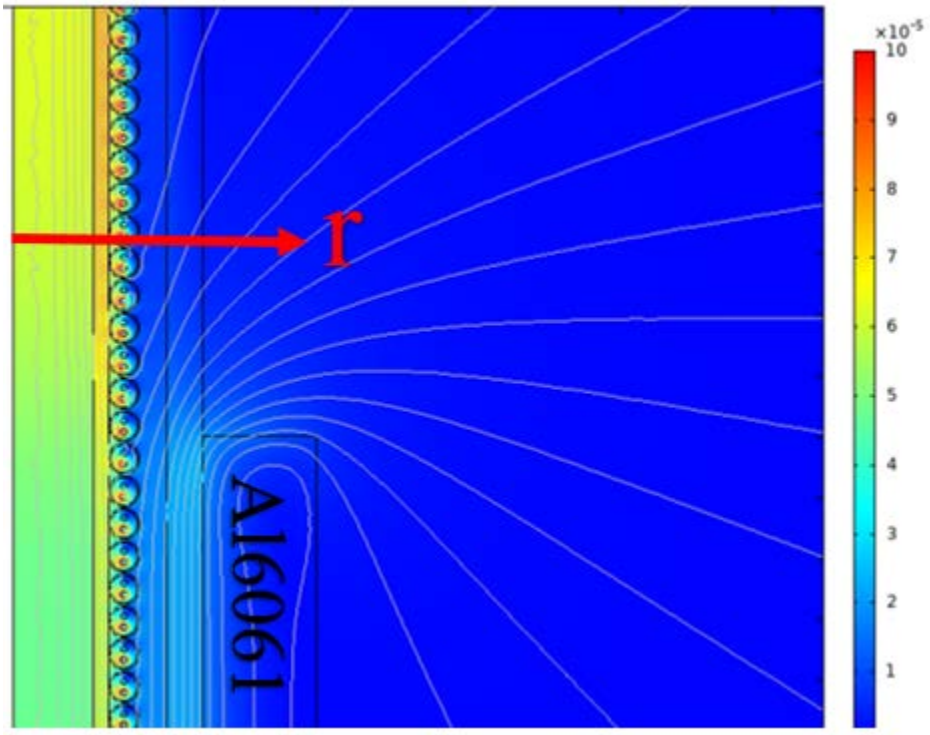

Figure 9: COMSOL generated map of magnetic field intensity.

Now that the model is believed to be running the appropriate physics, a mock calibration was simulated. This was accomplished by changing the model geometry such that the sensor moved axially to "see" different levels of the sodium analog. This mimics what is done experimentally as the winch system moves the sensor axially, while the test stand stays stationary. The results of the simulated calibration are compared to the experimental calibration to determine the accuracy of the model. Initially the results showed the simulated model under predicting the signal voltage, so model required tuning.

Several studies were conducted to determine the influence of varying different parameters in the model. The parameters were selected as they either had a range of values listed in literature, or the values are known to change due to environmental conditions. The parameters selected were the stainless steel permeability, the stainless steel conductivity, the process metal conductivity, and finally the orientation of the conductors. Following these studies, values for each parameter that agree with literature were selected to produce results that closely match what was observed experimentally. The results are presented in the next section.

8. Results

While exciting the primary coil, the secondary coil voltage was measured with a DMM that recorded data at one second intervals. Data was collected at each level increment for 300 seconds, and 100 data points were selected for processing around the median point of this 300 second period. The 100 data points were averaged and the mean was taken to represent the measurement at the corresponding level.

A method for refining the data called the "End Point Method" was used to produce a more accurate calibration [8]. This method assumes that measurements where the ends of the sensor coil are near the surface of the liquid metal are skewed due to the edge effects of electromagnetic interaction. If the ends of the sensor could can see a discontinuous section of metal (i.e. at the top of bottom of the "metal pool") the linear relationship between metal height and secondary output is disturbed. This effect skews the calibration curve, affecting the accuracy of the predicted sodium height. By removing the end points when generating a calibration curve, this skewing effect is lost. Data is presented in Figure 10.

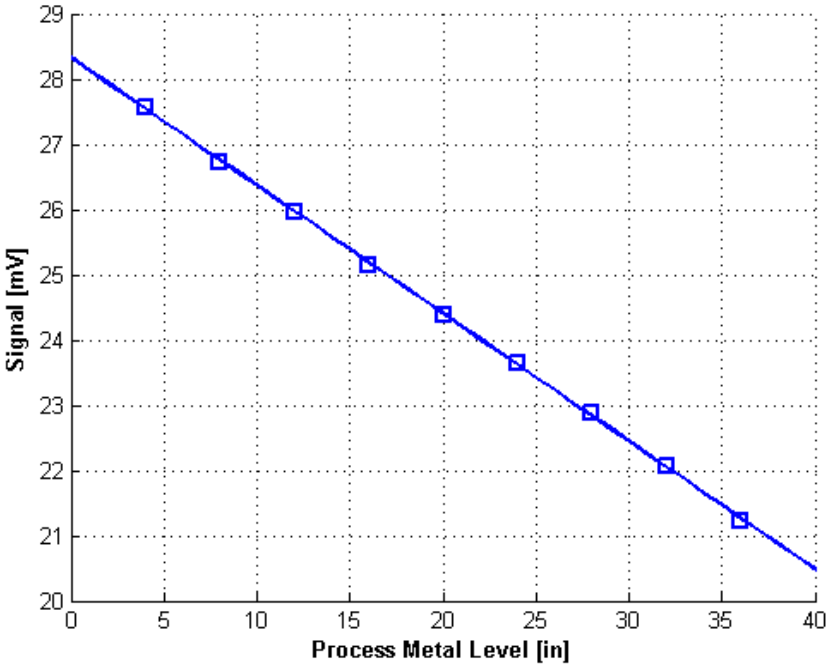

Figure 10: Experimental data collected in Testing Stand with MK-I Sensor

$$Signal = -0.196 * Level + 28.3217$$

$$R^2 = 0.9997$$

The resulting data shows a strong linear relationship between the height of the metal the sensor can see, and the secondary output voltage. This allows for a continuous measurement of metal level, as there is confidence in selecting values between the calibration data point.

The experimental calibration data is then compared to the results of the tuned COMSOL model. The COMSOL data is plotted in red over the experimental data in blue (Figure 11). An additional plot of the percent difference at each metal height is presented (Figure 12).

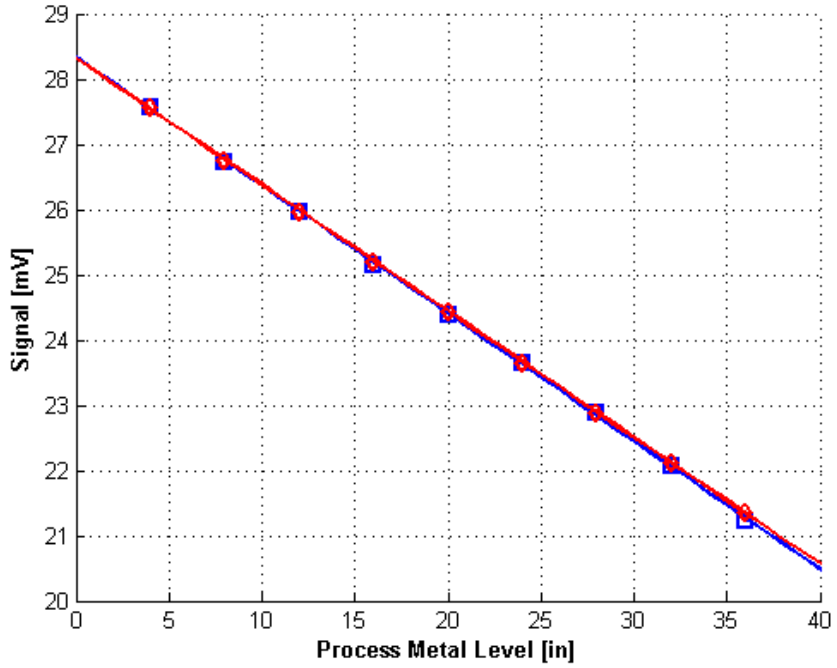

Figure 11: COMSOL generated calibration data overlaid on experimental calibration data

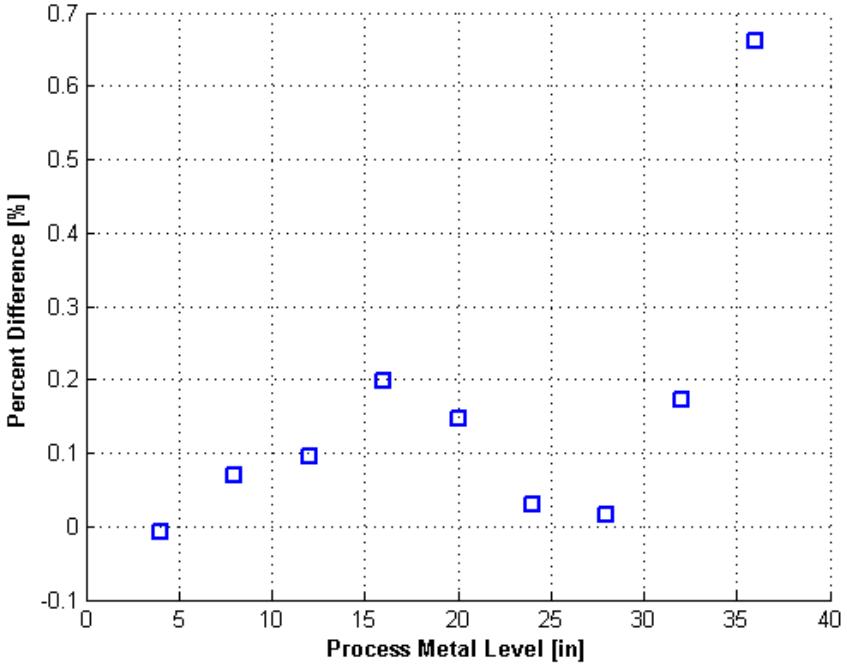

Figure 12: Percent difference between simulated data and experimental data

The above results show that the COMSOL model can closely predict the performance of the experimental sensor. This gives confidence that new sensor designs can be accurately modeled in COMSOL using the existing parameters.

Three parametric studies looking at material properties and their effect on sensor output are presented next. Each study has the sensor located such that it "sees" 20-inches of sodium, or the mid-point of the calibration curve. The first study examines the influence of the relative permeability of stainless steel on sensor output. This is important to examine as the cable sheath, sensor core, and sensor thimble are all constructed out of stainless steel. A range of 1.0 to 1.4 was selected based on findings in literature [6]. Results are presented in Figure 13.

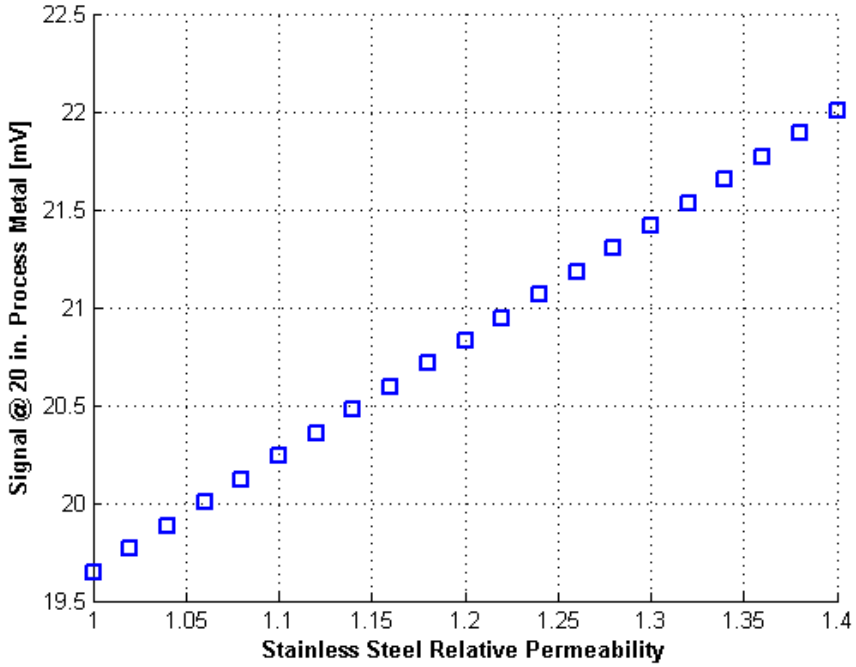

Figure 13: Change in sensor signal at 20" of process metal as a function of stainless steel relative permeability.

The second parametric study examined the influence the stainless steel conductivity has on sensor output. Again, the sensor design includes several components manufactured out of stainless steel so it is important to know how the material properties affect the results. The study tests the output of the sensor at 20-inches of metal, and the range used is 50% to 150% of the conductivity value found in literature [5]. Results are presented in Figure 14.

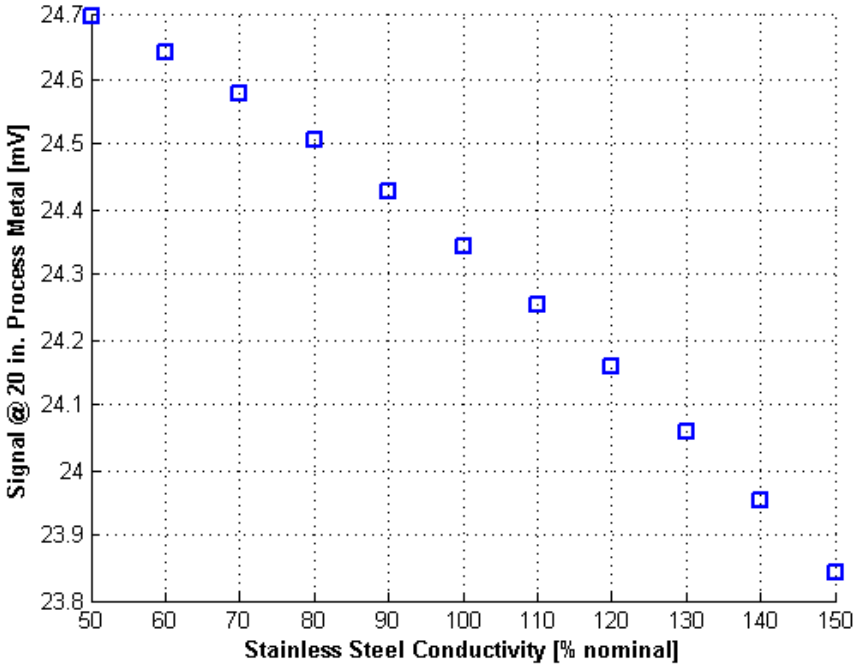

Figure 14: Change in sensor signal at 20" of process metal as a function of stainless steel electrical conductivity

The last parametric study examining the influence of material properties looks at the conductivity of the process metal, here Al6061. The eddy current effect this sensor utilizes is directly related to the electrical conductivity of the surrounding material. It is therefore important to quantify the influence this has on the sensor signal. The study tests the output of the sensor at 20-inches of metal, and the range used is 50% to 150% of the conductivity value found in literature [5]. Results are presented in Figure 15.

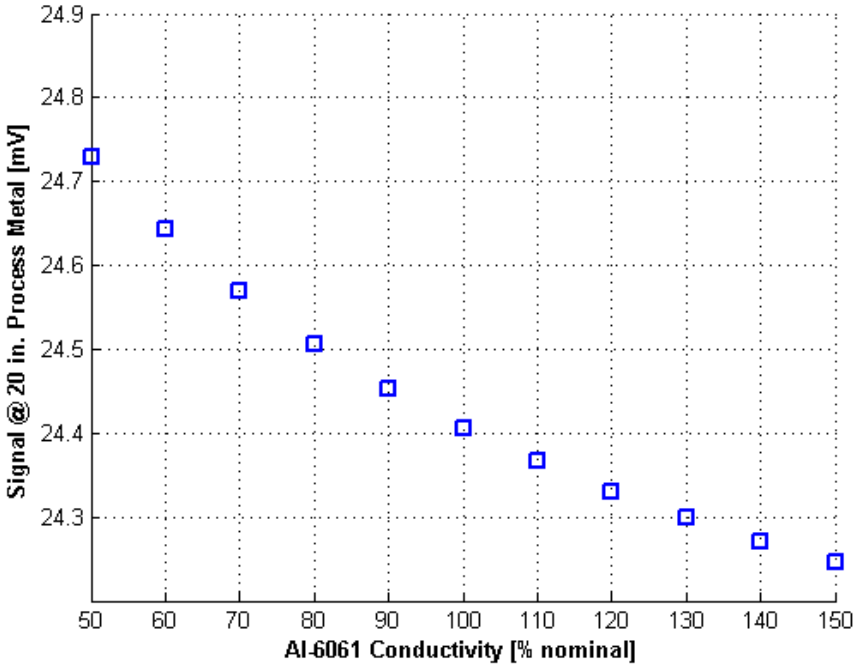

Figure 15: Change in sensor signal at 20" of process metal as a function of Al-6061 electrical conductivity

The final parametric study conducted during this work examines the effect of conductor orientation on the sensor output. When modeling the sensor, it became clear that the orientation of the two conductors inside the MI cable were essentially unknown. The conductors could be oriented vertically, horizontally, or some other arbitrary orientation. A study was then performed where the sensor was located at the 20-inch position and the orientation of the conductors inside the cable was rotated 360°. Results are presented in Figure 16.

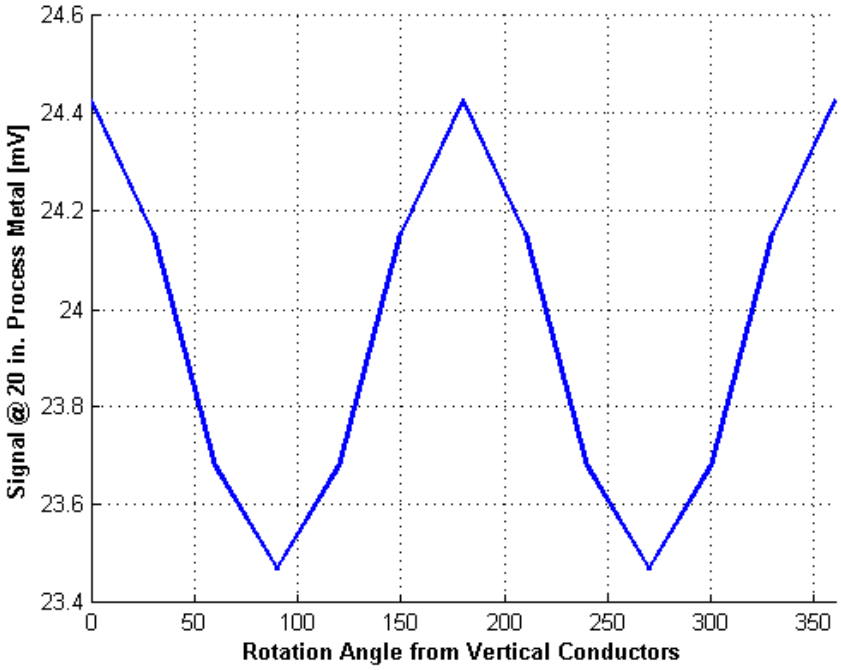

Figure 16: Change in sensor signal at 20" of process metal as a function of conductor orientation rotation.

The results of the last study show that the conductor orientation is critically important in properly validating the COMSOL model of this sensor's performance. The change in sensor signal caused by the rotation of the conductors is roughly the same magnitude as adjusting the conductivity of stainless steel or aluminum over the whole range examined above. As the experimental orientation cannot be determined without destroying the cable and sensor, a new design where the conductor orientation can be confidently determined is desired. Additionally, experimental measurements of the relative permeability and conductivity of the stainless steel and the conductivity of the Al6061 are desired to confidently input these values into COMSOL.

9. Updated Sensor Design

Following the experimental testing and COMSOL model validation there were several desirable design changes for the MILS-MK-II. The first was a move from two-conductor MI cable to a single-conductor MI cable. This greatly assists the modelling efforts as the orientation and geometry of each conductor is more quantifiable. This also makes the job of electrically terminating each conductor significantly easier, as the two-conductor cable had a tendency to short at the termination. Second was employing a bifilar wrapping method for the two, single-conductor cables. This again was aimed at making the modelling efforts easier, as the orientation of the conductors is better known. As the bifilar wrapping method produces half the number of wraps for each coil when compared to the two-layer wrapping, smaller cables and conductors were selected

for the MK-II design. Finally, the sensor core included features to better feed the cables to the top of the sensor, and a bottom guide was designed to align the sensor in the thimble. Figure 17 shows the 40-inch variation of the MILS-MK-II. Figure 18 shows a comparison between the wrapping of the MILS-MK-II and MILS-MK-I, as well as the bottom guide installed on the MILS-MK-II.

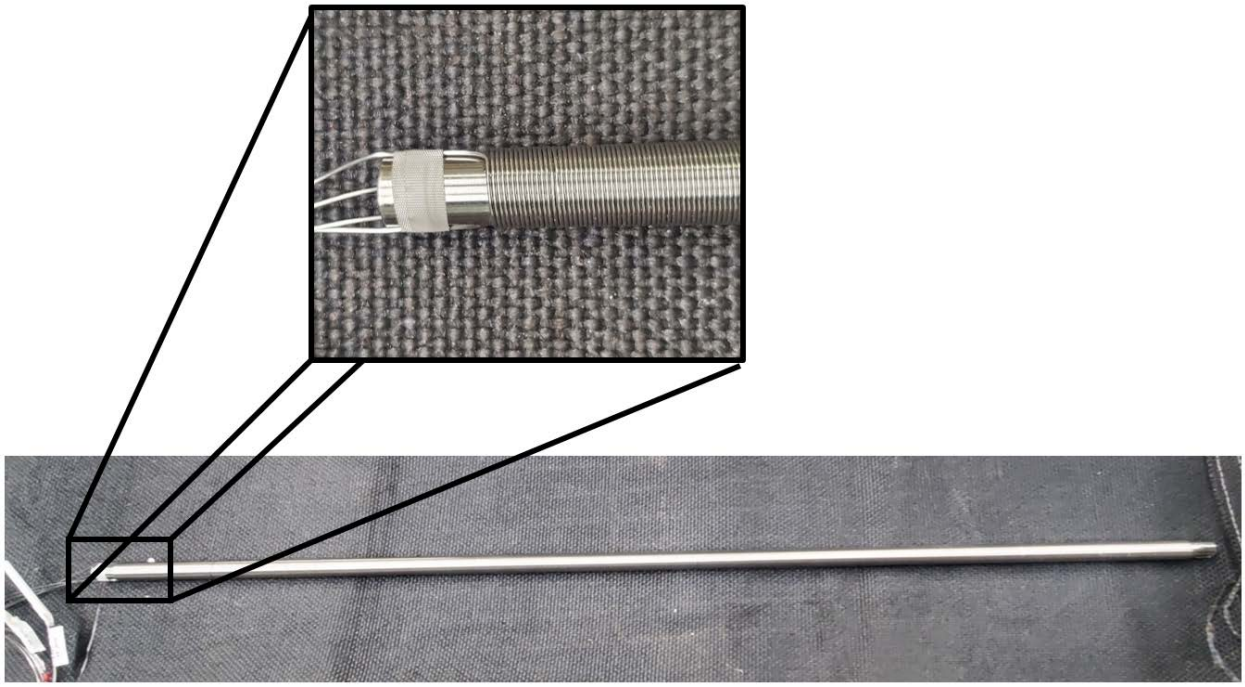

Figure 17: MILS-MK-II

Figure 18: Comparison of MILS-MK-II (left) with MILS-MK-I (right).

10.Sodium Testing

Sodium testing was performed in the METL Expansion Tank using the MILS-MK-I 70-inch variation. The use of the sealed thimble allowed for the sensor to be installed with the system hot and full of sodium. The sensor has operated in the METL Expansion Tank at 300°C for nearly a year with limited insulation degradation. The increase in operating temperature has increased the impedance of the sensor coils, but the effect was limited and has not changed since the initial heat up. An in-situ calibration has yet to be performed as the differential pressure level sensor also installed in the Expansion Tank plugged and is no longer available as a calibration comparison. A thermal rake level sensor will be installed in the Expansion Tank during the current METL shutdown that will provide an accurate calibration comparison with a 1-inch resolution. Following the in-situ calibration using the thermal rake, the MILS will be fully functional.

11.Conclusions and Path Forward

Revitalization efforts have produced mutually inductive level sensors capable of operating in liquid sodium up to 1000°F/538°C. Initial prototyping guided material selection and established operational experience. Two variations (MK-I and MK-II) of the MILS have been designed and fabricated using MI cable, and each has been sized for use in the METL Dump Tank as well as the Expansion Tank. One of these variations (MK-I) has seen over a year of operation in the METL Expansion Tank full of sodium at 300°C. The COMSOL Magnetic Fields Solver was used to simulate the operation of the MK-I design, and this model was used to guide the MK-II design. The MK-II design will next be commissioned in the non-sodium test stand located in building 308. Following this the commissioned sensors will be installed in METL where in-situ calibration will be performed to bring the sensors into normal operation.

12.Acknowledgements

This work is funded by the U.S. Department of Energy Office of Nuclear Energy's Advanced Reactor Technologies (ART) program. A special acknowledgement goes to Mr. Brian Robinson, Fast Reactor Program Manager for the DOE-NE ART program and to Dr. Robert Hill, the National Technical Director for Fast Reactors for the DOE-NE ART program for their consistent support of the Mechanisms Engineering Test Facility and its associated experiments, including the Inductive Level Sensor development. Prior years' support has also been provided by Mr. Thomas O'Connor, Ms. Alice Caponiti, and Mr. Thomas Sowinski of U.S. DOE's Office of Nuclear Energy.

13.References

[1] D. J. Griffiths, *Introduction to Electrodynamics*, Boston, MA, USA: Pearson, 2013
[2] J. D. Jackson, *Classical Electrodynamics*, New York, NY, USA: Wiley, 1999
[3] E. Kent, D. Kultgen, M. Weathered, C. Grandy, "Report on Level Sensor Development," ANL, Lemont, IL, USA: ANL-ART-163, ANL-METL-17
[4] O.J. Foust, *Sodium-NaK Engineering Handbook, Vol. 1, Sodium Chemistry and Physical Properties*, New York, NY, USA: Gordon and Breach, 1972
[5] J. R. Davis, "Engineering Data for Metals and Alloys," *Metals Handbook Desk Edition*, 2nd ed. Materials Park, OH, USA: ASM International, 1998, p 64-84
[6] N. G. Wilson and P. Bunch, "Magnetic permeability of stainless steel for use in accelerator beam transport systems," in *IEEE PAC*, San Francisco, CA, USA, 1991
[7] D. Kultgen et al., "Mechanisms Engineering Test Loop - Phase I Status Report - FY2018," ANL, Lemont, IL, USA: ANL-ART-148, ANL-METL-14
[8] H. W. Slocomb, "Liquid Metal Level Measurement (Sodium) State-of-the-Art Study," LMEC, Canoga Park, CA, USA, NAA-SR-Memo-12582
[9] USDOE NE Standard for Inductive Level Measurement Sensor For Use In Liquid Metal, NE C 5-1T, 1975, Cancelled 1996
[10] R. G. Geyer, *Dielectric Characterization and Reference Materials*, Gaithersburg, MD, USA: NIST, 1990

Nuclear Science and Engineering
Argonne National Laboratory
9700 South Cass Avenue, Bldg. 308
Argonne, IL 60439

www.anl.gov